Probing many-body localization in a disordered quantum magnet

D.M. Silevitch,[1] G. Aeppli,[2] and T. F. Rosenbaum[1,*]

[1]*Division of Physics, Mathematics, and Astronomy, California Institute of Technology, Pasadena, California 91125, USA*

[2]*Laboratory for Solid State Physics, ETH Zurich, Zurich, CH-8093, Switzerland; Dept. de Physique, EPF Lausanne, Lausanne, CH-1015, Switzerland; and Swiss Light Source, Paul Scherrer Institut, Villigen PSI, CH-5232, Switzerland*

Abstract

Excitations in disordered systems are typically categorized as localized or delocalized, depending on whether they entail disturbances extending throughout the system or are confined to small, generally nanometer scale, subsystems. Such categorization is impossible to achieve using traditional spectroscopy where the response to a weak oscillating (ac) electromagnetic probe is measured as a function of frequency. However, the localized excitations can be separated from each other as well as the delocalized continuum by measuring a spectral "hole" in the ordinary response while a large amplitude pump is imposed at a fixed frequency. Localized excitations will result in a very sharp "hole," and any residual couplings to other excitations, both localized and extended, will determine its detailed shape. This technique probes incoherent lifetime effects as well as coherent mixing or quantum interference phenomena, describable in terms of the Fano effect. Here we show that in a disordered Ising magnet, $LiHo_{0.045}Y_{0.955}F_4$, the quality factor Q for spectral holes, the ratio of the drive frequency to their width, can be as high as 100,000. In addition, we can tune the dynamics of the quantum degrees of freedom by sweeping the quantum mixing parameter through zero via the amplitude of the ac pump as well as a static external transverse field. The zero-crossing is associated with a dissipationless response at the drive frequency. The identification of such a point where localized degrees of freedom are minimally mixed with their environment in a dense and disordered dipolar coupled spin system implies control over the bath coupling of qubits emerging from strongly interacting many-body systems.

Popular Summary: Two important concepts associated with quantum states are coherence and interference. The first refers to the infinite lifetime of excited states of small, isolated quantum systems; the second to the representation of these states by waves that add to produce patterns with crests and troughs. Quantum systems composed of many atoms arranged imperfectly rarely illustrate these concepts. Our experiments demonstrate an exception in a disordered quantum magnet that divides itself into nearly isolated subsystems, i.e. displaying "many-body localization" These subsystems can be excited into a higher-energy state and tuned to have very long lifetimes. When they are in their excited quantum states, they display tunable wavelike interference. Such externally controllable, isolated subsystems reveal the ways in which many-body systems can be made to either couple to or decouple from their environment. Moreover, they have promise as quantum bits for future computers. They require less perfection than todays prototype quantum computers in cold atoms and solid state materials.

I. INTRODUCTION

Localization in quantum systems remains both fundamental to science as well as to technology. It is a venerable subject, starting with the work of Anderson[1]—whose name is associated with disorder-induced localization—and Mott, whose Mott localization transition[2] is due to repulsion between electrons. The combined problem of many-body localization[3–5] persists to this day, and recently has acquired practical relevance for systems of quantum devices. A notable example is the "D-wave" processor[6], which attempts to implement adiabatic quantum computation, but may be limited as a matter of principle by localization effects.

To control these long-lived and independent states, it is necessary to know how they interact with each other and with the outside world. Minimizing the interactions between coherent localized states and the continuum of states in the broader environment is an important goal for realizing an effective quantum computer[7–10]. However, these environmental couplings are by definition weak compared to the transitions among the states contributing to the spectrum for a particular localizing environment, making it difficult to study them directly. Recently, it has been posited that many weak couplings of this sort can be probed by pumping the system into a nonlinear response regime[11], saturating the discrete

transition associated with the coherent state, and using the emergence of a Fano resonance to characterize the interactions with the continuum states. In the present work, we use a magnetic adaptation of the Fano resonance technique to examine the coupling between coherent spin clusters quantum-mechanically isolated from the spin bath generated by other clusters of varying sizes. Our work differs from the experiments in quantum optics in that we are examining emergent degrees of freedom in a (magnetic) many-body system rather than single-particle states in atoms and semiconductor quantum dots. At the same time, it represents a major advance over our own previous activity on hole-burning in the same magnetic system in that we uncover a remarkably simple phenomenology, including the discovery of a zero-crossing for the Fano effect, as a function of non-linear drive amplitude and quantum mixing via a transverse field.

Asymmetric absorption lineshapes in atomic gases were first addressed by Ugo Fano more than 50 years ago[12]. They arise from interference between discrete transitions in the atoms and ionization into the continuum. Now known as Fano resonances, this formalism has found wide applicability in systems ranging from photo-ionized gases[13] to high-T_c superconductors[14] to photonic crystals[15] to quantum wells[16]. Their extension to spin liquids provides a means to characterize coherent spin clusters labeled in the time/frequency domain but distributed randomly in space.

II. REVIEW OF RELEVANT WORK ON $LiHo_xY_{1-x}F_4$

Spin clusters functioning as quantum two-level systems form in the dilute, dipolar-coupled magnet $LiHo_xY_{1-x}F_4$ under the appropriate thermodynamic conditions[17,18]. The magnetism in this family of rare-earth fluorides has long been studied as a realization of the dipole-coupled $S = 1/2$ Ising model, with the spins carried by the Ho^{3+} ions and the Ising axis lying along the crystallographic c axis[19,20]. The non-magnetic Y^{3+} ions randomly occupy the same sites as the magnetic Ho^{3+} ions with probability $1 - x$. The hierarchy of quantum levels accounting for the charge neutral excitations of individual Ho^{3+} ions (in the dilute limit where $x \ll 1$) of this wide-gap insulator has been summarized recently by Matmon et al.[21] Most relevant for the current low temperature study are the ground-state doublet for the Ising spins with a crystal field-derived 9.4 K gap to the first excited state and the hyperfine interaction between the electronic ($J = 8$) and nuclear ($I = 7/2$) spins of the

Ho^{3+} ions[19] that yields a nuclear Zeeman ladder consisting of eight states with spacing 0.2 K between consecutive levels. Analytic solutions of the microscopic Hamiltonian,[22–24] combined with measurements of the crystal-field parameters,[19,25] have quantitatively connected the microscopic Hamiltonian to the long-standing effective Hamiltonian for the spin physics. Magnetic fields applied perpendicular to the Ising axis mix the ground state doublet with the first excited state, inducing a splitting of the doublet which in the low field limit scales as $\Gamma = H_t^2$ (in contrast to the Zeeman splitting $\propto H_l$ of the ground state in a longitudinal field H_l) and leads to an effective transverse field Ising Hamiltonian[26,27]:

$$H = \sum_{i,j} J_{ij}\sigma_i^z\sigma_j^z - \Gamma\sum_i \sigma_i^x \tag{1}$$

In the pure ($x = 1$) limit, a classical ferromagnetic transition occurs at the Curie point $T_C = 1.53$ K dictated by the magnitude of the (predominantly) dipolar interactions J_{ij}. The quantum fluctuations induced by the transverse field disorder the Ising spins, producing a quantum critical point at $\Gamma = 1.6$ K where the Ising ferromagnetism vanishes. This zero temperature transition is linked by a line of second order transitions between paramagnetic and ferromagnetic phases to zero field. The principal features of the dynamics are propagating magnetic excitons[28].

While Eq. (1), which takes no account of the nuclear spins, is an excellent starting point for understanding the physics of pure $LiHoF_4$, at temperatures below ~ 0.6 K the electronic and nuclear spins of the Ho^{3+} ions[19] combine to form composite degrees of freedom with effective spins $I + J$, resulting in an upturn in the ferromagnet-paramagnet phase boundary for pure $LiHoF_4$[27]. Furthermore, entanglement of the nuclear and electron spins results in an incomplete softening of the principal excitonic mode at the quantum phase transition[25,28].

Additional physics has been revealed at holmium concentrations between $x = 1$ for the pure ferromagnet and the $x \ll 1$ dilute ion limit[29]. The combination of disorder, the magnetic dipole interaction, which can be ferromagnetic or antiferromagnetic (depending on the relative orientation of the preferred spin direction and the vector separating two spins), and quantum fluctuations[30–32] creates a sequence of states as a function of decreasing dipole (Ho) concentration[29], progressing from mean-field ferromagnet[27] to random-field ferromagnet[33] to spin glass[26,34–36] to spin liquid[17]. Here, we focus on the Bhatt-Lee spin-liquid[37] (originally proposed for phosphorus-doped silicon near its metal-insulator transition) for $x \sim 0.05$ and weak thermal coupling, characterized by a hierarchy of singlets derived from combinations

of doublets (isolated spins) and triplets (ferromagnetically coupled spins). The hierarchy of singlets results in a low frequency susceptibility which scales as $1/T^{\alpha}$ with $\alpha \neq 1$ rather than following Curie or spin-glass forms. For $LiHo_{0.045}Y_{0.955}F_4$, α was experimentally measured to be 0.75, less than the Curie exponent $\alpha = 1.0$ due to the compensation of spins by each other as they form singlets on cooling[38].

III. HOLE BURNING AND LOCALIZATION IN DISORDERED QUANTUM SPIN SYSTEMS

Fig. 1a shows schematically how a disordered quantum spin system such as $LiHo_xY_{1-x}F_4$ at low concentrations or Si:P[37,39] breaks into decoupled clusters and isolated spins, focusing on some clusters, whose classical ground states are ferromagnetic but which because of small transverse fields imposed by other clusters, can be described as two-level systems with low-energy eigenstates which are coherent superpositions of up and down configurations $|\Uparrow\rangle \pm |\Downarrow\rangle = |\uparrow\uparrow\cdots\uparrow\rangle \pm |\downarrow\downarrow\cdots\downarrow\rangle$[17]. For simplicity, we do not consider electronuclear spin mixing which will introduce a more elaborate level scheme[28,40] at low energies because this does not qualitatively change the physics of hole burning which we seek to outline in this section. In the limit where these degrees of freedom are independent, the effective low-energy Hamiltonian is $H_{\rm le} = \sum_i H_i$ with

$$H_i = \Delta_i \sigma_i^x + M_i h(t) \sigma_i^z, \tag{2}$$

where the sum is over decoupled clusters i characterized by an underlying moment M_i and pseudospin operators σ_i, Δ_i correspond to the splitting between the two states $|\Uparrow\rangle \pm |\Downarrow\rangle$ for cluster i, and $h(t)$ is an external drive field. If $h(t)$ is a time-independent constant $h > 0$, the magnetization normalized to M_i is

$$\langle \sigma_i^z \rangle = \frac{h^2 M_i^2 + \lambda_i M_i h}{\lambda_i^2 + \lambda_i M_i h}, \tag{3}$$

where $\lambda = \sqrt{\Delta_i^2 + h^2 M_i^2}$. For $h \ll \lambda_i$, $\langle \sigma_i^z \rangle = M_i^2 h/\Delta_i$ while for $h \gg \lambda_i$, we obtain the expected saturation magnetization of unity. Now we consider an oscillating field $h(t) = h\cos(\omega t)$ where for all i, $\hbar\omega \ll \lambda_i$. The full magnetization in this case will then merely be $M(t) = \sum_i M_i \langle \sigma_i^z \rangle \cos(\omega t)$. If we relax the condition on $\hbar\omega$ but insist that the drive

amplitude $h \ll \Delta/M_i$, we obtain the usual linear response form

$$M(t) = \sum_i M_i^2 h \left(\frac{\Delta_i}{\Delta_i^2 - (\hbar\omega)^2} \cos(\omega t) \right) + \sin(\omega t) \left(\delta(\hbar\omega - \Delta_i) - \delta(\hbar\omega + \Delta_i) \right) \qquad (4)$$

where there is now an out-of-phase response which if the frequency is scanned gives the density of states, weighted by M_i^2 for the clusters.

Once we see a continuum in the out-of-phase linear response for a many-body system, a priori we do not know whether we are dealing with a sum of spectra of localized subsystems, as in Eq. (2), for which the eigenfunctions are simply given by direct products of the wavefunctions for the subsystems, or if we are dealing with shorter-lived excitations whose behavior is dominated by coupling between subsystems. A standard method in spectroscopy to determine whether a continuum is due to independent—i.e. localized—two-level systems is to simultaneously relax the conditions on ω and h to enter the more interesting and heavily studied regime of driven two-level systems. The idea is to apply a large amplitude field at frequency $\hbar\omega = \Delta_i$ so that $\langle \sigma_i^z(t) \rangle$ has oscillations of sufficiently large amplitude so that further increments in field can yield only small increases in $\langle \sigma_i^z \rangle$. Without delving into the mathematics of the time-dependent Schrdinger equation[41] for the Hamiltonian (1), one can convince oneself (a) of the plausibility of this given the magnetization saturation with increasing h in the static limit described by Eq. (3). At the same time, (b) the resonant enhancement of the linear response (4) for ω near $\Delta_i/\hbar$ indicates that we can preferentially excite subsystems i with $\omega = \Delta_i$. (a) and (b) together lead to the conclusion that the sample becomes more transparent to radiation at the drive frequency, and a sharp hole is burnt into the spectrum if the two-level system in question cannot interact with two level systems with other values of Δ_i. If such spectral holes can be found in an interacting many-body system, then we can speak about the system exhibiting many-body localization in the sense of having excited states which are direct products of the excited states for subsystems, meaning that the entire system cannot act as its own heat bath. If there is a weak residual coupling between subsystems, the holes will acquire shapes with width parameters which measure that weak coupling.

IV. EXPERIMENTS ON $LiHo_xY_{1-x}F_4$

For $LiHo_{0.045}Y_{0.955}F_4$ both the thermal link to the heat bath[18] and magnetic fields applied transverse to the Ising axis[42] control the observability of localized excited states. In particular, strong coupling to a thermal bath yields the linear response expected from a spin-glass[18,35], no observable localized excited states, and consequently no evidence for the Fano resonance is seen for weak coupling (Fig. 1d). We therefore concentrate here on weak coupling to the bath. We cooled a single crystal of $LiHo_{0.045}Y_{0.955}F_4$ in a helium dilution refrigerator and measured its ac magnetic susceptibility for frequencies from 1 to 2000 Hz. The thermal coupling between the crystal and the heat reservoir—the mixing chamber of the dilution refrigerator—was in the "weakly coupled" regime described by Ref. 18, thereby maximizing quantum fluctuations. We employed a pump-probe technique[17,18,42] to access the nonlinear response regime. In this configuration, a two-frequency ac magnetic field is applied along the Ising axis of the crystal. A strong (0.2-0.6 Oe) field $h_{\rm pump}\cos(2\pi f_{\rm pump}t)$ excites clusters at the pump frequency $f_{\rm pump}$. Simultaneously, a 20 mOe probe field is swept through a range of frequencies to yield a linear response from the crystal. The net response of the crystal is then sensed by an inductive pickup coil. Due to the extremely narrow separation between the pump and probe frequencies (as small as 1 mHz), disentangling the responses required the development of a 2-stage lock-in technique, where the combined response is passed into a commercial lock-in amplifier tuned to the probe frequency, and the resulting output is sampled by a computer and passed through a software lock-in detector tuned to $\Delta f = f_{\rm pump} - f_{\rm probe}$. It should be noted that the sampling step requires a minimum of $1/\Delta f$ seconds; all of the data reported here were sampled for a minimum of $2/\Delta f$ seconds.

The first step in the measurements is to determine pump fields $h_{\rm pump}$ sufficient to enter the non-linear regime. Fig. 1c shows the magnitude and phase angle of the magnetization induced for a range of frequencies $f_{\rm pump}$, limited to a maximum of 10 Hz to allow measurement to drive fields above 1 Oe without excessive eddy current heating. The data generally follow an S-shaped curve, whose inflection point moves outward with increasing frequency, in agreement with the model (2) where the longitudinal field couples the localized singlet ground state of a cluster to an excited state separated by a small gap[38]; the susceptibility at higher frequencies is more sensitive to smaller clusters where the gap is larger, which can only be overcome by a higher drive field $h_{\rm pump}$. For our pump-probe experiments we

operate near to and somewhat above the inflection point; very high driving fields are avoided because they lead to excessive heating. While the system consists of an ensemble of spin clusters with a broad range of sizes, choosing a particular pump frequency selects for a set of clusters which are similarly sized and hence sorted by resonant frequency.

We turn now to pump-probe measurements, examples of which are shown in Fig. 2a. The characteristic asymmetric shape of a Fano resonance is immediately obvious, providing a direct indication of a weak coupling between the coherent spin cluster and the continuum of surrounding spin states (Fig. 1b,c). As the temperature is increased, the amplitude of the resonant response drops, and the resonance appears to broaden, with the response suppressed to 8% of its original amplitude at $T = 500$ mK and to below the noise floor of the measurement at 700 mK. Given that the overall linear susceptibility of $LiHo_{0.045}Y_{0.955}F_4$ has a strong temperature dependence, the thermal evolution of the resonant response can be seen more clearly by normalizing it to the linear response at each temperature (determined by measuring $\chi''(\Delta f = 30\text{ mHz})$). We show in Fig. 2b spectra obtained at a series of temperatures, normalized, and then combined into a surface plot where color and height now represent the absorption for a given Δf and T. The broadening of the resonance with increasing temperature emerges clearly in this visualization, and we examine it quantitatively in Fig. 2c by looking at the evolution of the linewidth in the fits to the Fano form,

$$\chi''(\Delta f) = A\frac{(\frac{q\Gamma}{2} + \Delta f)^2}{\Delta f^2 + \frac{\Gamma^2}{2}} \tag{5}$$

where Γ is the linewidth of the resonance and q, known as the Fano parameter, characterizes the interference between the different transition pathways. The mHz scale low-temperature limit of the linewidth suggests that the coupling between the clusters and the background spin bath is weak, and hence that the system can be considered in the framework of a 2-level system in weak contact with the environment rather than a continuous relaxation process. Quantum states with splittings substantially smaller than nominal bath temperatures are very common in solids and liquids, and indeed form the basis for various resonance (e.g. NMR) spectroscopies, many of which rely on non-equilibrium quantum state preparation. Reduced bath coupling during cool-down increases the T_1 and T_2 times associated with such quantum states, and so makes a description of the magnetic response of the system as due to a set of independent multilevel quantum systems more appropriate than a picture based on classical, thermal diffusion.

When a multi-level quantum description applies, for a fixed bath coupling (which extracts heat) and ac driving field (which inserts heat), an equilibrium with a set of fixed state occupancies will characterize the system, and to first order the equilibrium can be described by a fixed effective temperature. On the other hand, the non-equilibrium dynamics are dominated by small multilevel systems describable in terms of some generalized Bloch equation, exactly as is the case e.g. for NMR performed even at room temperature, and are therefore quantum mechanical. The linewidth increases exponentially with T, consistent with a thermally activated process with a gap $\Delta = 740$ mK, which is an energy of order near neighbor spin couplings, but well below the first excited crystal field state energy and above the bandwidth associated with the nuclear hyperfine interactions. The gap energy is also large compared to the < 1 mK characteristic energy of a single Ho^{3+} ion magnetized by a 0.3 Oe field, indicating that the resonances are not due to single-spin behavior but instead are consistent with a picture consisting of clusters of > 100 spins behaving as a large effective 2-level system protected from others in a wavefunction such as that $|\Uparrow\rangle \pm |\Downarrow\rangle = |\uparrow\uparrow\cdots\uparrow\rangle \pm |\downarrow\downarrow\cdots\downarrow\rangle$ (discussed above) at low temperatures because of a relatively large single spin flip energy. In addition to the thermal broadening of the resonance, the interaction between the cluster and the spin bath also responds to temperature. We plot in Fig. 2d the lineshape asymmetry, $q(T)$. q increases approximately linearly with temperature for $T < 0.25$ K, plateauing above that point. A possible microscopic origin for this behavior is that as the temperature grows, thermally activated spin flips will occur within clusters containing antiferromagnetically coupled spins. Such spin flips will result in increased dipolar moments for the clusters, and thus an increased coupling to remanent dipole moments of the other clusters forming the underlying "bath", an effect also seen in the temperature-dependent linewidth shown in Fig. 2c. To rephrase, heating begins to unbind the clusters and so reveals them to each other. Provided that a single constant J_{AFM} characterizes the underlying antiferromagnetic coupling, we would find that for $k_B T \gg J_{AFM}$ the probabilities that two spins are either ferromagnetically or antiferromagnetically correlated become equal and we would see a plateau in the coupling to other clusters as well as the value q. Such plateaus also can be found if there is a discrete series of antiferromagnetic couplings $J_{AFM,i}$ and the conditions $J_{AFM,i} \ll k_B T \ll J_{AFM,i+1}$ are met. The discrete nature of the distribution of dipolar couplings for the $LiHo_xY_{1-x}F_4$ lattice leads to the possibility that these conditions obtain, and therefore the data in Fig. 2d, which extend only as far as hole burning can be seen (and q

can be measured), could be a manifestation of such a plateau.

It should be noted that the "free-induction" relaxation time of $\sim 10-30$ seconds observed previously[17] is substantially shorter than the $\sim 500-1000$ seconds of the inverse linewidth of the hole uncovered in the driven pump-probe measurements. This follows because the "free induction decay" was measured for relaxation after the strong ac drive field was turned off, while the linewidth here is measured in the far more weakly driven linear regime. More formally, the rotating wave approximation[41] does not apply for the combination of strong (non-linear) drive fields and low frequency employed for our experiments. In particular, the Rabi frequency $f_{\rm Rabi}$ associated with the 0.5 Oe drive field $h_{\rm pump}$ for the electronic (Ising-like) spin of a single Ho^{3+} ion is $g_{||}\mu_B h_{\rm pump} \sim 10\,{\rm MHz} \gg f_{\rm pump}$, which is precisely opposite to the requirement that $f_{\rm Rabi} \ll f_{\rm pump}$ for the rotating wave approximation to hold.

We explore in Figs. 3 and 5 the effects of changing the amplitude of the pumping field. Most important is the change in sign of the Fano q: for the largest drive field (0.5 Oe) the low and high frequency responses are enhanced and suppressed, respectively, opposite to what we see for the lower drive field. The zero crossing of q occurs at a critical $h_{\rm pump} = 0.45$ Oe. The data points at the pump frequency at which pump and probe-derived signals cannot be distinguished are ignored for the Fano fits because they represent the response of the highly excited (pumped) clusters and not the perturbatively mixed clusters with other resonant frequencies.

The upper and lower frames of Fig. 5 reveal clear distinctions between $\chi_{\rm drive}$, the total signal at $f = f_{\rm pump}$ and $\chi_{\rm Fano}$, the linear Fano contribution calculated from evaluation at $f = f_{\rm pump}$ of the fitted Fano form to data at $f \neq f_{\rm pump}$. First, $\chi'_{\rm drive}$ goes through a maximum at the zero-crossing of q, while $\chi'_{\rm Fano}$ undergoes a decrease which looks like a rounded step. Second, when we plot the phases $\phi = \tan^{-1}\chi''/\chi'$, we find that while both $\chi_{\rm drive}$ and $\chi_{\rm Fano}$ have phase shifts which are smaller at high $H_{\rm drive}$, the latter actually has a zero near the zero of q. In other words, for small linear perturbations, the Fano response is dissipationless in the limit $f \to f_{\rm pump}$. This result follows from Eq. 5, which gives $\phi = \phi(q) = \tan^{-1}\frac{q^2}{1-q^2}$, a functional form that we superpose over the experimental results in the lower frame of Fig. 5. The absence of dissipation in the Fano response that describes the linear continuum at $q = 0$ means that hole burning is actually complete at the drive frequency: there is no continuum contribution to χ'' which remains unaffected by the drive in the limit $f \to f_{\rm pump}$. Significantly, the absence of dissipation at the q zero crossing indicates that the clusters can

be largely protected from decohering interactions with the environment by application of a macroscopic tuning parameter. While $\phi(q)$ gives a rough account of the experimental phase angle as q moves away from zero, the data ultimately deviate from $\phi(q)$, which implies that some oscillators even with frequencies close to $f_{\rm pump}$ are not contributing to the Fano profile.

Varying the ac pump amplitude accesses different mixtures of the states of the localized clusters. The additional power applied to the drive solenoid also results in eddy-current induced heating of the copper susceptometer mount, and hence some degree of conductive heating of the sample despite the low-thermal-conductivity Hysol epoxy spacers holding the sample inside the susceptometer. This, as well as dissipation within the sample itself, gives rise to a higher effective temperature, with a concomitant loss of coherence. The decoherence of the resonant excitation is reflected by a measurable increase in the linewidth Γ, whose temperature-dependent evolution can be traced readily in Fig. 2c. Over the range of pump amplitudes shown in Fig. 3, the resonance linewidth increases from 1.1 mHz to 1.8 mHz (Fig. 5a), equivalent to approximately 50 mK of direct thermal heating. Even while heating is clearly present, the line widths remain negligible on the scale of the drive frequency, allowing the coherent superpositions of the cluster and continuum oscillations. Their relative signs change at a critical longitudinal pump field of 0.45 Oe, thus yielding the zero crossing of q, one of the main results of our experiment.

We now take advantage of one of the key features of the Li(Ho,Y)F_4 family, the ability to tune the microscopic Hamiltonian by applying a magnetic field transverse to the Ising axis, thereby quantum-mechanically mixing the single ion and cluster eigenstates[22,26] via different matrix elements than does the ac longitudinal field. Nonetheless, application of a transverse field induces a crossover (Fig. 4) at a well-defined crossover field of $H_t = 3.5$ kOe[42], similar to that seen earlier as a function of pump amplitude (Fig. 3). We plot in Fig. 6c the transverse field dependence of the Fano parameter q. This parameter changes linearly with H_t over most of the experimental range, showing that the external transverse field not only changes the energies of different states, but also tunes their interactions with the broader spin bath environment. In particular, at the $H_t = H_c = 3.5$ kOe crossover field, q vanishes, opening the possibility for the static transverse field to be used to largely decouple excited states from the spin bath. At the same time, as also seen when we varied $h_{\rm pump}$ to obtain a zero-crossing of q, the phase has a quadratic zero in phase for $\chi_{\rm Fano}(f_{\rm pump})$ and a maximum in $\chi'_{\rm drive}$, both of which coincide with the zero of q and can be roughly described by the

function $\phi(q)$. However, in contrast to what we saw for the $h_{\rm pump}$ scan with $H_t = 0$, $\chi'_{\rm drive}$ and $\chi'_{\rm Fano}$ are nearly indistinguishable at $f_{\rm pump}$. Another contrast, anticipated from the previous paragraph and visible in the comparison of Figs. 5a and 6a, is that the linewidth is, to within error, H_t-independent. The essentially constant behavior of the linewidth is a strong indication that the evolution due to the transverse-field-induced quantum fluctuations is fundamentally different from the purely classical behavior seen as a function of increasing temperature.

V. DISCUSSION

The ability to tune the interaction between the excited clusters and the spin bath without introducing dissipation establishes $LiHo_{0.045}Y_{0.955}F_4$ as a fruitful macroscopic system for investigating localized many-body states with weak and tunable coupling to the environment[3]. In fact, it has been suggested[43,44] that MBL effects would be observable in such systems via detailed measurements of the energy spectra of spatially localized operators. Recent experiments in cold-atom systems[45,46] have addressed similar questions in lower dimensions, employing the degree of disorder rather than the strength of the coupling to the external environment as the principal tuning parameter.

The field scale H_c can be connected with the microscopic behavior of Li(Ho,Y)F_4 by comparison with an exact diagonalization of the full Hamiltonian for a pair of coupled Ho^{3+} atoms[24], where there is a crossing of the lowest coupled electro-nuclear levels for nearest-neighbor spins positioned in the ab plane at (100) or (010) relative to each other. The effects of these pairwise level crossings can be seen in the measured linear longitudinal susceptibility $\chi_{zz}(H_t)$[24,42]. The characteristic dynamics of the pairwise susceptibility shift as a function of classical (temperature) and quantum-mechanical (transverse field) energy scales, moving from 0.9 T at 70 mK to 0.5 T at 150 mK. We expect the same level crossings to impact the dynamics of the larger spin clusters addressed by the pump-probe measurements described here.

We have characterized here the Fano resonances inserted by a nonlinear drive field into the continuum of magnetic excitations in a dense set of interacting dipoles. The resonances are remarkably narrow ($Q = \frac{f_{\rm pump}}{\Gamma} = \frac{202\,{\rm Hz}}{2\,{\rm mHz}} \approx 10^5$), implying that excitations in this medium are strongly localized, notwithstanding the long range and large strength of the dipolar

interaction. The large but finite lifetime of the excitations is due to a slight mixing between these (almost perfectly) localized excitations and the continuum formed by their ensemble. This manifests itself in the Fano q, which measures the interference between processes taking the ground state of a localized subsystem to an excited state either directly or via another (nearly) localized subsystem[47]:

$$q = \frac{M_{g\alpha} + \mathbb{P}\sum_k \frac{M_{gk}V_k}{\hbar\omega - E_k}}{\pi \sum_k M_{gk}V_k \delta(\hbar\omega - E_k)}, \tag{6}$$

where $M_{g\alpha} = \langle g|M|\alpha\rangle$ and $M_{gk} = \langle g|M|k\rangle$ are the matrix elements connecting the ground state to the discrete excited state and to the continuum, respectively, and V_k is the matrix element connecting the discrete excited state to the kth continuum state, which has energy E_k[47]. Inspection of Eq. 6 allows us to start to understand one of the key results of our experiment, namely the zero crossing of q. In the nonlinear regime, the numerator has a modified matrix element $M_{g'\alpha'}$ describing how the longitudinal magnetic field couples the ground and excited states g' and α' as modified by the drive field from g and α, while the denominator contains the product of the analogous matrix element M_{gk} for off-resonant pairs of ground and excited states and the hopping terms V_k between the resonant and off-resonant excited states. It is unlikely that the off-resonant M_{gk} will be much changed by external ac and dc fields, and so—assuming that the principal value term in the numerator cancels to zero—sign changes in q follow from a sign change either in $M_{g'\alpha'}$ or in V_k. A sign change in the latter actually would imply a zero in the former as well because without such a zero, q would diverge at the critical pump (Fig. 5) or transverse (Fig. 6) field h_c. Where all terms in Eq. 6 are analytic near the zero crossing, and with the knowledge that q is linear in h_{pump} and H_t near the zero crossing, we can draw a sharper conclusion, namely that $M_{g\alpha}$ scales like $(h-h_c)^{(n+1)}$ if V_k scales like $(h-h_c)^n$. This means that as h_{pump} crosses h_c, the incremental magnetization δM due to mixing of ground $g(h)$ and excited $\alpha(h)$ states moves from in-phase to out-of-phase with small additional drive fields δh. It is reasonable to believe that where this occurs, the incremental magnetization due to the changing occupancies of the ground and excited states will be highest so that as we observe in the experiment, the zero crossing of q will coincide with the maximum of the total susceptibility which sums diagonal (state occupancy-dominated) and off-diagonal ($M_{g\alpha}$-dominated) contributions. A further consequence of such considerations is that as the off-diagonal matrix element $M_{g\alpha}$ which accounts for the Fano effect grows from zero, it will also account for an ever larger fraction

of the dissipation measured directly at the pump frequency. This allows the proposal of a phenomenological form (solid blue line) for the phase angles plotted in Figs. 5d and 6d:

$$\phi'(q) = \tan^{-1}\left(\frac{q^2}{q^2 + c^2 + (h_{\rm pump}/d)^2} \cdot \frac{\chi''_{\rm drive}(f = f_{\rm pump})}{\chi'_{\rm drive}(f = f_{\rm pump})}\right), \tag{7}$$

where $c = 0.12$ represents the intrinsic contributions of the off-diagonal matrix element and $d = 1.4$ Oe incorporates the thermal effects associated with changes in pump amplitude.

VI. CONCLUSIONS

Via hole burning, we have demonstrated localization of excitations among interacting magnetic dipoles. For strong coupling to the heat bath, previous work has shown a trend towards spin freezing at low temperatures[18,35], and the current work (Fig. 1d) shows no spectral hole burning in this strong coupling limit, corresponding to delocalized excitations. Reducing the coupling to the bath induces a transition to a spin liquid state[18,38] where the excitations are localized to a very high degree, with a $Q \sim 10^5$ for the spectral hole. The small mixing between excited states of different spin clusters leads to a Fano effect, whose phenomenology for this complex system is remarkably simple, with a vanishing q coinciding with an inflection point in the ac magnetization induced by the drive field responsible for the hole-burning. The ability to tune the interactions between the spin clusters and the background spin bath, and in particular the appearance of a dissipation-free state at the point where q vanishes, suggests a new avenue for creating long-lived quantum states with minimal decoherence and environmental coupling. The experiments show the value of hole-burning for characterizing many-body localization[3–5], and also demonstrate how nonlinear quantum dynamics can reveal emergent two-level systems.

We thank G. Refael and Markus Müller for helpful discussions. The work at Caltech was supported by US Department of Energy Basic Energy Sciences Award de-sc0014866.

---

* Email: tfr@caltech.edu

[1] P. W. Anderson, Physical Review **109**, 1492 (1958).

[2] N. F. Mott, Proceedings of the Physical Society. Section A **62**, 416 (1949).

[3] R. Nandkishore and D. A. Huse, Annual Review of Condensed Matter Physics **6**, 15 (2015).

[4] D. A. Huse, R. Nandkishore, V. Oganesyan, A. Pal, and S. L. Sondhi, Physical Review B **88**, 014206 (2013).

[5] D. M. Basko, I. L. Aleiner, and B. L. Altshuler, Annals of Physics **321**, 1126 (2006).

[6] M. W. Johnson, M. H. S. Amin, S. Gildert, T. Lanting, F. Hamze, N. Dickson, R. Harris, A. J. Berkley, J. Johansson, P. Bunyk, E. M. Chapple, C. Enderud, J. P. Hilton, K. Karimi, E. Ladizinsky, N. Ladizinsky, T. Oh, I. Perminov, C. Rich, M. C. Thom, E. Tolkacheva, C. J. S. Truncik, S. Uchaikin, J. Wang, B. Wilson, and G. Rose, Nature **473**, 194 (2011).

[7] T. Pellizzari, S. A. Gardiner, J. I. Cirac, and P. Zoller, Physical Review Letters **75**, 3788 (1995).

[8] M. S. Byrd and D. A. Lidar, Physical Review Letters **89**, 047901 (2002).

[9] A. M. Tyryshkin, S. A. Lyon, W. Jantsch, and F. Schäffler, Physical Review Letters **94**, 126802 (2005).

[10] G. Ithier, E. Collin, P. Joyez, P. J. Meeson, D. Vion, D. Esteve, F. Chiarello, A. Shnirman, Y. Makhlin, J. Schriefl, and G. Schön, Physical Review B **72**, 134519 (2005).

[11] M. Kroner, A. O. Govorov, S. Remi, B. Biedermann, S. Seidl, A. Badolato, P. M. Petroff, W. Zhang, R. Barbour, B. D. Gerardot, R. J. Warburton, and K. Karrai, Nature **451**, 311 (2008).

[12] U. Fano, Physical Review **124**, 1866 (1961).

[13] H. C. Bryant, B. D. Dieterle, J. Donahue, H. Sharifian, H. Tootoonchi, and D. M. Wolfe, Physical Review Letters **38**, 228 (1977).

[14] C. Thomsen, M. Cardona, B. Gegenheimer, R. Liu, and A. Simon, Physical Review B **37**, 9860 (1988).

[15] A. N. Poddubny, M. V. Rybin, M. F. Limonov, and Y. S. Kivshar, Nature Communications **3**, 914 (2012).

[16] J. Faist, F. Capasso, C. Sirtori, K. West, and L. Pfeiffer, Nature **390**, 589 (1997).

[17] S. Ghosh, R. Parthasarathy, T. F. Rosenbaum, and G. Aeppli, Science **296**, 2195 (2002).

[18] M. A. Schmidt, D. M. Silevitch, G. Aeppli, and T. F. Rosenbaum, Proceedings of the National Academy of Sciences **111**, 3689 (2014).

[19] P. Hansen, T. Johansson, and R. Nevald, Physical Review B **12**, 5315 (1975).

[20] P. Beauvillain, J. P. Renard, I. Laursen, and P. J. Walker, Physical Review B **18**, 3360 (1978).

[21] G. Matmon, S. A. Lynch, T. F. Rosenbaum, A. J. Fisher, and G. Aeppli, Physical Review B **94**, 205132 (2016).

[22] P. B. Chakraborty, P. Henelius, H. Kjonsberg, A. W. Sandvik, and S. M. Girvin, Physical Review B **70**, 144411 (2004).

[23] M. Schechter, Physical Review B **77**, 020401 (2008).

[24] C. M. S. Gannarelli, D. M. Silevitch, T. F. Rosenbaum, G. Aeppli, and A. J. Fisher, Physical Review B **86**, 014420 (2012).

[25] H. M. Rønnow, J. Jensen, R. Parthasarathy, G. Aeppli, T. F. Rosenbaum, D. F. McMorrow, and C. Kraemer, Physical Review B **75**, 054426 (2007).

[26] W. Wu, B. Ellman, T. F. Rosenbaum, G. Aeppli, and D. H. Reich, Physical Review Letters **67**, 2076 (1991).

[27] D. Bitko, T. F. Rosenbaum, and G. Aeppli, Physical Review Letters **77**, 940 (1996).

[28] H. M. Rønnow, R. Parthasarathy, J. Jensen, G. Aeppli, T. F. Rosenbaum, and D. F. McMorrow, Science **308**, 389 (2005).

[29] D. H. Reich, B. Ellman, J. Yang, T. F. Rosenbaum, G. Aeppli, and D. P. Belanger, Physical Review B **42**, 4631 (1990).

[30] J. Brooke, T. F. Rosenbaum, and G. Aeppli, Nature **413**, 610 (2001).

[31] M. Schechter and P. C. E. Stamp, Physical Review Letters **95**, 267208 (2005).

[32] D. M. Silevitch, G. Aeppli, and T. F. Rosenbaum, Proceedings of the National Academy of Sciences **107**, 2797 (2010).

[33] D. M. Silevitch, D. Bitko, J. Brooke, S. Ghosh, G. Aeppli, and T. F. Rosenbaum, Nature **448**, 567 (2007).

[34] S. M. A. Tabei, M. J. P. Gingras, Y.-J. Kao, P. Stasiak, and J.-Y. Fortin, Physical Review Letters **97**, 237203 (2006).

[35] J. A. Quilliam, S. Meng, C. G. A. Mugford, and J. B. Kycia, Physical Review Letters **101**, 187204 (2008).

[36] K.-M. Tam and M. J. P. Gingras, Physical Review Letters **103**, 087202 (2009).

[37] R. N. Bhatt and P. A. Lee, Physical Review Letters **48**, 344 (1982).

[38] S. Ghosh, T. F. Rosenbaum, G. Aeppli, and S. Coppersmith, Nature **425**, 48 (2003).

[39] M. A. Paalanen, T. F. Rosenbaum, G. A. Thomas, and R. N. Bhatt, Physical Review Letters **48**, 1284 (1982).

[40] R. Giraud, W. Wernsdorfer, A. M. Tkachuk, D. Mailly, and B. Barbara, Physical Review Letters **87**, 057203 (2001).

[41] P. Hanggi, in *Quantum Transport and Dissipation* (Wiley VCH Verlag GmbH, Weinheim, 1998) pp. 249–286.

[42] D. M. Silevitch, C. M. S. Gannarelli, A. J. Fisher, G. Aeppli, and T. F. Rosenbaum, Physical Review Letters **99**, 057203 (2007).

[43] S. Johri, R. Nandkishore, and R. N. Bhatt, Physical Review Letters **114**, 117401 (2015).

[44] M. H. Fischer, M. Maksymenko, and E. Altman, Physical Review Letters **116**, 160401 (2016).

[45] M. Schreiber, S. S. Hodgman, P. Bordia, H. P. Lüschen, M. H. Fischer, R. Vosk, E. Altman, U. Schneider, and I. Bloch, Science **349**, 842 (2015).

[46] J.-y. Choi, S. Hild, J. Zeiher, P. Schauß, A. Rubio-Abadal, T. Yefsah, V. Khemani, D. A. Huse, I. Bloch, and C. Gross, Science **352**, 1547 (2016).

[47] D. M. Riffe, Physical Review B **84**, 064308 (2011).

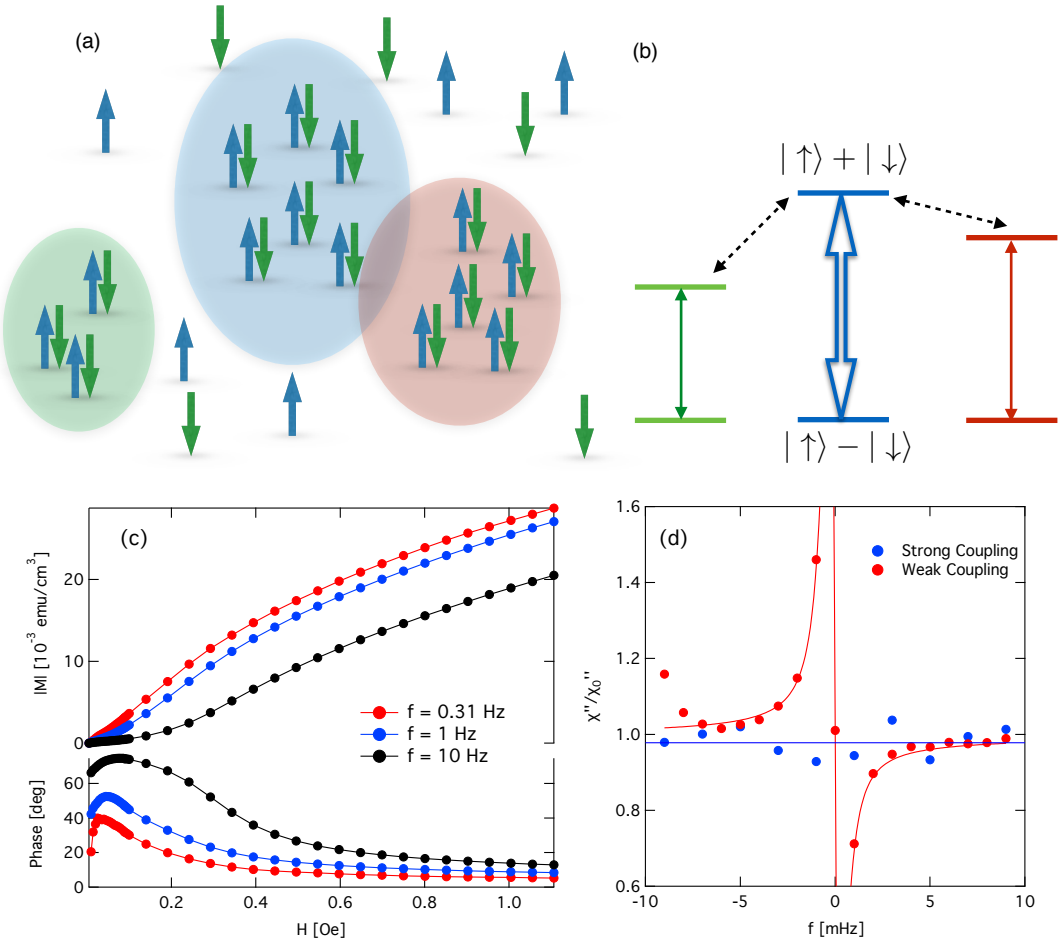

FIG. 1. Schematic of spin configuration and transition pathways in pumped $LiHo_{0.045}Y_{0.955}F_4$. (a) Tightly-bound spin clusters embedded in a dilute spin bath. Closely-separated spins form a tightly bound cluster which can be magnetized in a nonlinear response regime by a strong ac pump field. Spatially adjacent clusters can interact directly. (b) Schematic of cluster excitation pathways. Clusters of different sizes have different energy gaps, so choice of pump frequency acts as a size selector. Direct interactions between excited clusters and off-resonance clusters give rise to Fano resonance behavior. (c) Magnetization amplitude (top) and phase angle (bottom) for three different excitation frequencies. (d) Pump-probe measurements in two thermodynamic limits. When $LiHo_{0.045}Y_{0.955}F_4$ is weakly coupled to an external heat reservoir, the low temperature state is dominated by the cluster response, giving rise to strong Fano resonances. When it is strongly coupled to an external heat reservoir, it exhibits extended glassy behavior including the absence of hole-burning and Fano resonance effects[18]. Both traces were measured at $T = 100$ mK, $f_{\rm pump} = 20$ Hz, and $h_{\rm pump} = 0.5$ Oe.

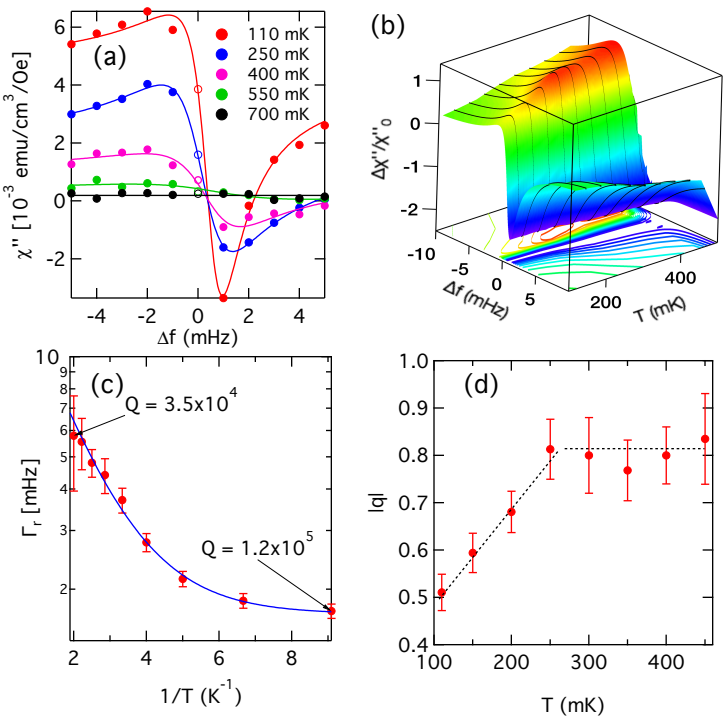

FIG. 2. Linear absorption spectra of $LiHo_{0.045}Y_{0.955}F_4$ as a function of temperature; excitation field has 20 mOe amplitude. (a) Measured absorption in the presence of a 0.3 Oe pump field at $f_{\rm pump} = 202$ Hz and zero transverse field. Curves are fits to Fano resonance forms, Eq. 5 in the text. The points at $f = f_{\rm pump}$ (open symbols) are omitted from the fits (see text for details). (b) Absorption normalized with respect to the response at $\Delta f = 30$ mHz as a function of frequency and temperature. (c) Linewidth of the resonance, as determined from fitting to the Fano model, vs. temperature T. Line is a fit to an intrinsic linewidth of 1.7 mHz plus exponential thermal broadening with $\Delta = 740$ mK. (d) Fano parameter q vs. temperature, showing the suppression of coupling to the bath at the lowest T. Lines are guides to the eye.

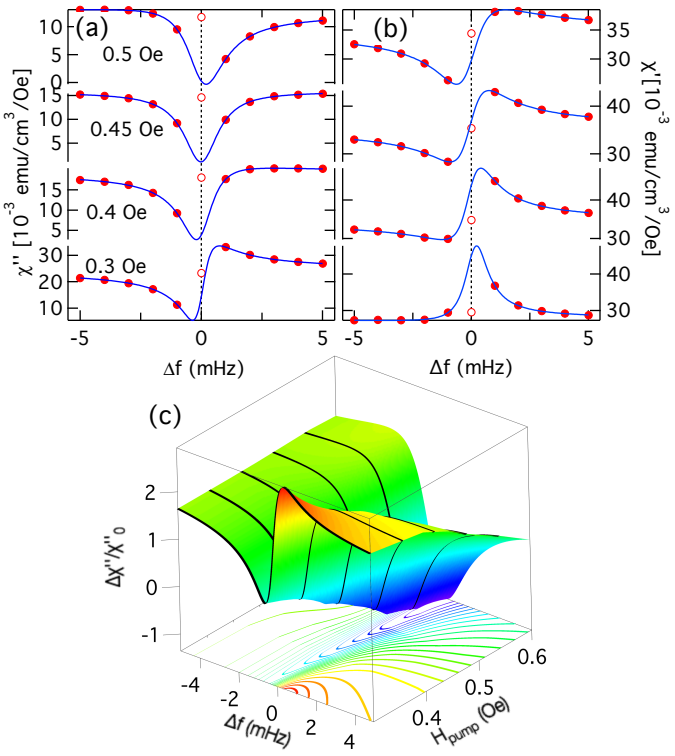

FIG. 3. Linear absorption as a function of pump amplitude at $T = 0.11$ K for a 202 Hz pump. (a,b) Measured imaginary and real susceptibilities (points), and fits to a Fano resonance form as a function of pump amplitude at zero transverse field. Increasing the pump amplitude tunes the resonant behavior, at the cost of increased decoherence. (c) Normalized absorption as a function of frequency and pump amplitude.

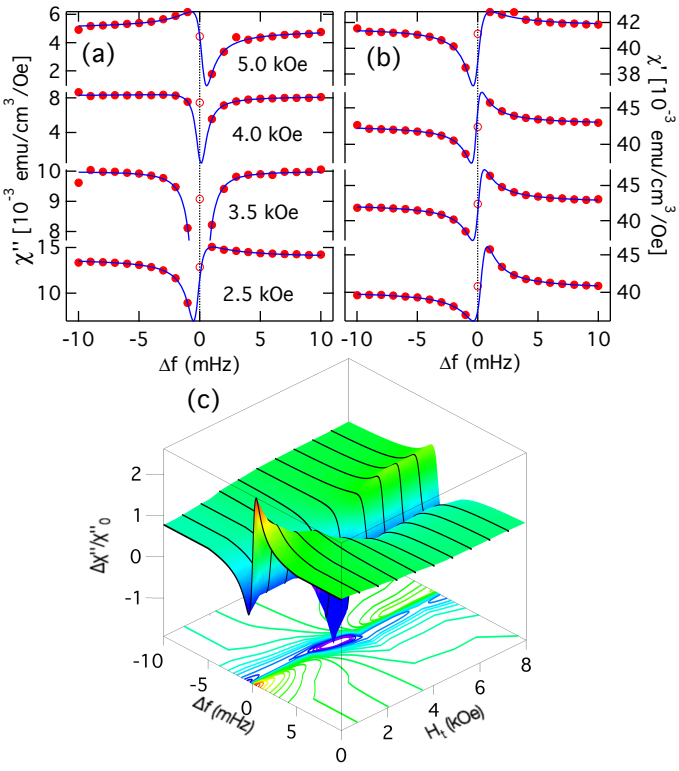

FIG. 4. Linear absorption as a function of transverse field at $T = 0.11$ K for a 202 Hz pump (a,b) Measured imaginary and real susceptibilities (points) and fits to a Fano resonance as a function of transverse field for a fixed 0.3 Oe pump. Transverse field-induced quantum tunneling tunes the resonant behavior without a corresponding increase in decoherence. (c) Normalized absorption as a function of frequency and transverse field.

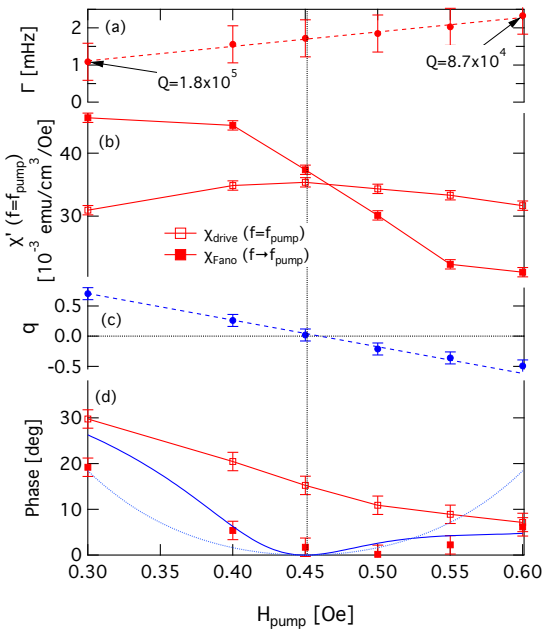

FIG. 5. Evolution of resonant behavior as a function of pump amplitude. (a) Fano linewidth Γ vs. ac drive $h_{\rm pump}$; increasing the drive amplitude broadens the linewidth and hence reduces the oscillator Q. (b) Real susceptibility χ' measured directly at $f = f_{\rm pump}$ (open symbols) and determined by extrapolating the fitted Fano resonance to $f = f_{\rm pump}$ (filled symbols), showing the contrast in behavior between the nonlinear and linear responses respectively. (c) Fano parameter q vs. drive amplitude showing a continuous evolution including a smooth crossing through zero. Dashed line is a guide to the eye. (d) Evolution of the phase of the complex susceptibility at $f = f_{\rm pump}$ for the nonlinear (open symbols) and linear (filled symbols) responses. The zero crossings of q are associated with a local minimum in the dissipation, and a corresponding minimum in the phase shift of the linear probe response as the probe frequency approaches the pump frequency. $\phi(q) = \tan^{-1}\frac{q^2}{1-q^2}$(blue dotted curve) follow from Eq. 5 in the text, while the solid blue curve (see Eq. 7 and associated discussion in text) provides a better description of the experimental data.

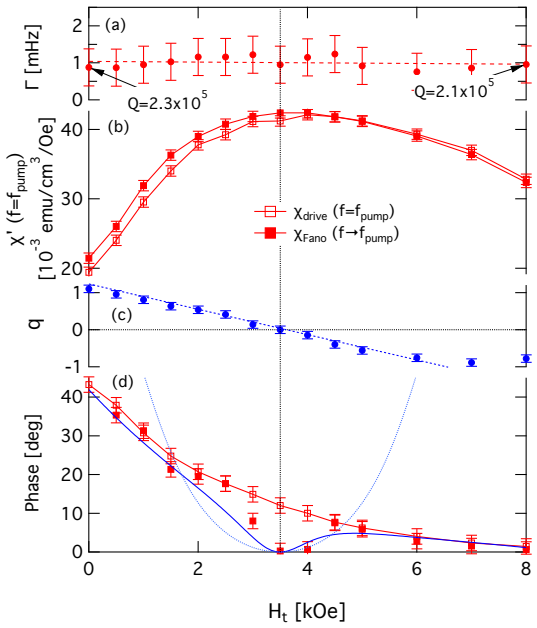

FIG. 6. Evolution of resonant behavior as a function of transverse field. (a) Fano linewidth Γ vs. transverse field; in contrast to the behavior as a function of $h_{\rm pump}$, increasing H_t does not change the linewidth. (b) Real susceptibility χ' measured directly at $f = f_{\rm pump}$ (open symbols) and determined by extrapolating the fitted Fano resonance to $f = f_{\rm pump}$ (filled symbols), showing a small but clearly apparent distinction in the evolution of the nonlinear and linear responses. (c) Fano parameter q vs. transverse field showing a continuous evolution including a smooth crossing through zero. Dashed line is a guide to the eye. (d) Evolution of the phase of the complex susceptibility at $f = f_{\rm pump}$ for the nonlinear (open symbols) and linear (filled symbols) responses. As with the $h_{\rm pump}$ dependence shown in Fig. 5, the zero-crossing of q is associated with a vanishing of the dissipation in the linear response with the same functional form, demonstrating universal behavior from two disparate tuning parameters.